UNIVERSITY OF LEEDS

This is a repository copy of *A Fractal Interpretation of Archie-like Equation for Partially Saturated Porous Media*.

White Rose Research Online URL for this paper:
https://eprints.whiterose.ac.uk/id/eprint/226566/

Version: Accepted Version

Article:
Wei, W., Hu, X., Cai, H. et al. (4 more authors) (2025) A Fractal Interpretation of Archie-like Equation for Partially Saturated Porous Media. Journal of Geophysical Research: Solid Earth, 130 (6). e2024JB030619. ISSN 2169-9313

https://doi.org/10.1029/2024JB030619

This is an author produced version of an article published in Journal of Geophysical Research: Solid Earth made available under the terms of the Creative Commons Attribution License (CC-BY), which permits unrestricted use, distribution and reproduction in any medium, provided the original work is properly cited.

Reuse
This article is distributed under the terms of the Creative Commons Attribution (CC BY) licence. This licence allows you to distribute, remix, tweak, and build upon the work, even commercially, as long as you credit the authors for the original work. More information and the full terms of the licence here: https://creativecommons.org/licenses/

Takedown
If you consider content in White Rose Research Online to be in breach of UK law, please notify us by emailing eprints@whiterose.ac.uk including the URL of the record and the reason for the withdrawal request.

White Rose university consortium
Universities of Leeds, Sheffield & York

eprints@whiterose.ac.uk
https://eprints.whiterose.ac.uk/

A Fractal Interpretation of Archie-like Equation for Partially Saturated Porous Media (Revised)

Wei Wei[1], Xiangyun Hu[1†], Hongzhu Cai[1], Jianchao Cai[1,3,†], Paul W.J. Glover[2], Piroska Lorinczi[2], and Qi Han[1]

[1]School of Geophysics and Geomatics, China University of Geosciences, Wuhan, China

[2]School of Earth and Environment, University of Leeds, Leeds, UK

[3]State Key Laboratory of Petroleum Resources and Prospecting, China University of Petroleum, Beijing 102249, China

†Corresponding author: Xiangyun Hu (xyhu@cug.edu.cn), Jianchao Cai (caijc@cug.edu.cn)

Note: words/sentences/paragraphs in blue indicate revisions or newly-added material.

Key points:

- An electrical conductivity model for partially saturated porous media is derived under the assumption that surface conductivity is negligible.
- Physical definitions of the saturation exponent in Archie equation are proposed.
- A new form of Archie equation is introduced by incorporating with the cementation exponent and the saturation exponent.

Abstract

The complex mechanism by which the conducting phase in pore space influences the electrical conductivity of rocks has been a critical focus in geophysical exploration. In this study, the Pore-Solid Fractal model is used to accurately describe the fluid distribution within pore space, and the resistivity index follows a form analogous to Archie equation, being expressed in terms of the tortuosity fractal dimension, the pore fractal dimension, and saturation. The physically-based fractal parameters then determine the saturation exponent. We find a reasonable prediction for experimental data with a feasible parameter linking the cementation exponent and the saturation exponent. Furthermore, the interrelationship between cementation exponent and saturation exponent is also analysed under various conditions. An alternative expression for the exponents is introduced, exhibiting good agreement with experimental measurements. Additionally, a bound model is presented in order to address the uncertainty of tortuosity due to uncertainties of the tortuosity fractal dimension during the saturating process. The boundary is a useful constraint on the range of the resistivity index, particularly in cases where structural parameters are insufficiently constrained.

Plain Language Summary

In the realm of geophysical exploration, predicting the microstructural properties and fluid distribution characteristics (e.g., porosity and saturation) of rocks based on electrical conductivity data presents a formidable challenge. Fortunately, electrical conductivity follows a clear power-law relationship with porosity and saturation when plotted logarithmically for reservoir rocks. Nevertheless, its exponents, known as the cementation exponent and saturation exponent, are typically treated as empirical parameters. To explore the physical meaning of these exponents, we present a theoretical electrical conductivity model in power-law form using fractal geometry. The model is then analysed for different water contents. We find that these exponents are functions of fractal dimension, which describes the extent to which an object fills space whilst exhibiting similar forms. A simplified expression of these exponents reveals the factors controlling the variation of electrical conductivity with porosity and saturation. Due to the similarity in form, we also infer the relationship between the cementation exponent and the saturation exponent, and introduce a bound model to constrain the range of the electrical conductivity based on porosity and saturation. This model helps simplify the process of predicting electrical conductivity by reducing uncertainties associated with empirical parameters.

1. Introduction

Characterizing pore structure and fluid distribution using electrical data is essential for estimating transport characteristics of rocks, such as permeability [*Niu and Zhang*, 2019], capillary pressure [*Rashid et al.*, 2015; *Li et al.*, 2019], streaming and zeta potential [*Walker and Glover*, 2018; *Peng et al.*, 2019], electrical conductivity and ionic diffusion [*Jougnot et al.*, 2009], thermal conductivity [*Revil*, 2000] and the different transport properties [*Hamamoto et al.*, 2010]. The electrical conductivity of rock is highly dependent on the distribution of aqueous fluids within their complex pore systems [*Norbisrath et al.*, 2015]. Moreover, electrical conductivity is easier to measure in the laboratory compared to other transport properties, especially for rock samples with low permeability and porosity [*Garing et al.*, 2014]. Since the electrical conductivity of rocks varies over many orders of magnitude, it serves as a highly sensitive probe for changes in water-saturated pore volume [*Greve et al.*, 2013; *Glover*, 2015]. Archie equations and their generalizations [*Glover et al.*, 2000; *Glover*, 2010], as empirical models, are widely applied in well logging and reservoir exploration [*Niu and Zhang*, 2018]. The dimensionless resistivity index (I) is related to fluid saturation (S_w) and saturation exponent (n), which reflects how resistivity changes with varying saturation levels. The saturation exponent (n) is typically determined by fitting resistivity measurement data obtained from partially saturated sandstone cores [*Glover*, 2017],

$$I = S_w^{-n} \tag{1}$$

Equation (1) matches most experimental data from conventional reservoir rocks without accounting for surface electrical conductivity [*Balberg*, 1986]. A detailed theoretical discussion of the interpretation of n, including its dependence on pore structure and fluid distribution can be found in [*Glover*, 2015; 2017]. The definition of "fluid distribution" refers to the spatial arrangement of the wetting and non-wetting fluids within the pore space, influenced by factors such as pore size, connectivity, capillary forces, and wettability. However, the impact of fluid distribution on electrical resistivity is not fully understood [*Mustofa et al.*, 2022], leading to the extrapolation of

n without a coherent physical interpretation.

In previous work, we proposed an electrical conductivity model for fully saturated fractal porous media based on fractal geometry and the tortuous capillary model [*Wei et al.*, 2015]. In this model, the pore fractal dimension (D_F) describes the fractal distributions of pore size, while the tortuosity fractal dimension (D_T) characterizes the fractal distribution of electrical tortuosity [*Duy Thanh et al.*, 2019]. The strong agreement between the *Wei et al.* [2015] model and published data demonstrates that these two fractal parameters effectively describe electrical conduction in a fully saturated pore space with conducting fluid. Partial saturation of pore space leads to a more complex and disconnected conductive system [*Glover*, 2010]. As a result, the *Wei et al.* [2015] model cannot represent the increased tortuosity of the conductive phase under partially saturated conditions.

Several fundamental theories are used to analyse the fluid distribution in pore space and its effect on electrical conductivity. These include percolation theory [*Hunt et al.*, 2014], effective medium theory [*Ghanbarian-Alavijeh and Hunt*, 2012], critical path analysis approach [*Friedman and Seaton*, 1998; *Ghanbarian and Sahimi*, 2017] and fractal theory [*Cai et al.*, 2017; *Rembert et al.*, 2020; *Wang and Revil*, 2020]. Percolation theory describes the formation of connected fluid pathways within a porous medium, which is crucial for understanding how fluids are distributed and flow through the pore network, especially near critical saturation thresholds [*Hunt et al.*, 2014]. Additionally, combining percolation theory with the effective medium approach enables the characterization of conductivity under different saturation levels, including universal scaling [*Cai et al.*, 2017]. The Pore-Solid Fractal (PSF) model, a detailed application of fractal theory in partially saturated pore spaces, has been developed to characterize fluid distribution in porous media [*Perrier et al.*, 1999; *Bird et al.*, 2000; *Ghanbarian-Alavijeh and Hunt*, 2012]. The model characterizes pore size distribution, where the wetting fluid preferentially occupies smaller pores due to capillary forces. The pore system follows a natural fractal structure, with fluid distributed across the fractal pore network based on standard assumptions.

A more detailed description of the PSF model was provided by *Perrier et al.* [1999]

and *Bird et al.* [2000]. *Bird et al.* [2000] presented a solid-fluid distribution model based on the PSF structure at the Represent Element Volume (REV) scale,

$$\theta=\phi-\kappa\left[1-\left(\frac{r_{\max}}{r}\right)^{D_F-D_E}\right] \tag{2}$$

here, θ is water content (i.e., water phase fraction, $\theta=\phi S_w$), and ϕ is porosity (fractional); D_F is the pore fractal dimension of the pore space (typically $2 \leq D_F \leq 3$ in many geological materials), D_E is the Euclidean dimension of the embedding space; r and $r_{\max}$ are pore diameter and the maximum pore diameter (or the REV size), respectively; κ is an empirical parameter that modifies the water content based on the fractal structure. In many cases, κ values range from 0.2 to 0.8 [*Perrier et al.*, 1999; *Bird et al.*, 2000], which can be taken approximately equal to ϕ to simplify the calculation, indicating that the "effective" fluid portion scales proportionally to the total porosity. For example, the model accurately matches the experimental data in predicting the primary wetting and drying branches of soil-water retention curves [*Ojeda et al.*, 2006; *Wang et al.*, 2020].

A key issue with Archie empirical parameters is the unknown relationship between cementation exponent (m) and saturation exponent (n), though both are described in the same terms by the Generalised Archie's law relative to different reference frames [*Glover*, 2010].

The original values of m and n in Archie equation for sandstone were derived from the fitted slope of a log-log plot of resistivity versus porosity or saturation [*Archie*, 1942]. Several improvements and discussions regarding Archie equation have been made to better understand the inherent meaning of these parameters [*Coleman and Vassilicos*, 2008; *Yue and Tao*, 2013; *Glover*, 2016]. However, a universal expression for electrical conductivity in both fully and partially saturated porous media is still lacking, making the accurate determination of m and n challenging [*Mohamad and Hamada*, 2017]. However, using the bounds model we can calculate the upper and lower bounds of electrical conductivity with porosity and saturation [*Cai et al.*, 2017]. For example, Archie equation can be viewed as a combination of parallel, random, and perpendicular conductivity models. Additionally, *Glover* [2010; 2016; 2017] extended Archie model to account for two conducting phases, where each phase has its own

exponent that describes its level of connectivity. Glover's model can also be extended to three or more phases, making it suitable for analysing the electrical properties of sedimentary rock with more complex mineral compositions.

This work utilizes the PSF model, and combined with previous research on saturated porous media [*Wei et al.*, 2015], to present an electrical conductivity model for fractal porous media under partial fluid saturation. The empirical parameter n is analysed in terms of its physical significance, particularly in relation to fractal dimensions. The validity of the model is demonstrated using four sets of resistivity-saturation experimental data, encompassing a total of 90 samples. Furthermore, the integrated electrical conductivity model is applied to analyse the direct relationship between m and n. Finally, a bound model is discussed to define the upper and lower of the resistivity.

2. Model Development

2.1 Resistivity index-saturation model based on PSF model

Figure 1 shows the development of a PSF model from a multi-phase porous medium. Figure 1(a) shows the initial two-dimensional image with the solid matrix represented by white, and porosity shown in black. If a grey phase is added, the black and grey together represent porosity, with the two colours distinguishing different fluid phases, such as water and gas. This type of medium can be effectively described using the PSF model. The PSF model is a standard multi-phase fractal model, which can be seen as an extension of the Sierpinski carpet in two-dimensional space (Figure 1(b)) or the Menger sponge in three-dimensional space. In the PSF model (Figure 1(c)), the fluid phase serves as the iterative element used to generate both the pore and solid phases. Therefore, the equation derived from the two-phase fractal model can be extended into the form of a PSF model.

In previous work, we systematically analysed the correlation between electrical conductivity and other physical parameters, describing how tortuosity (τ) varies with scale (i.e., characteristic unit length, λ) and with the tortuosity fractal dimension (D_{Tp}) [*Wheatcraft and Tyler*, 1988; *Guarracino et al.*, 2014],

$$\tau(\lambda) = \left(\frac{L_0}{\lambda} \right)^{D_{Tp}-1} \tag{3}$$

where L_0 is defined as the length of the saturated porous media, representing the reference "straight line" length of the current path. The parameter L_0 also defines the upper limit to the scale range for fractal behaviour.

If Equation (2) satisfies the condition that $\kappa = \phi$ when r becomes significantly smaller than $r_{\max}$ [*Bird et al.*, 2000], then Equation (2) can be replaced with the following expression,

$$\theta = \phi \left(\frac{r_{\max}}{r} \right)^{D_F - D_E} \tag{4}$$

Consequently, Equation (4) holds under the condition that $r << r_{\max}$. As r approaches $r_{\max}$, the assumption $\kappa = \phi$ breaks down, rendering Equation (4) invalid.

For a porous medium fully saturated with brine, the formation factor F, defined as the ratio of the electrical conductivity of the liquid phase to that of the rock, is related to the pore tortuosity τ_p and porosity ϕ [*Perkins et al.*, 1956],

$$F = \frac{\tau_p^{\,2}}{\phi} \tag{5}$$

Traditionally, the formation factor is not applied in partially saturated systems. However, the definition we have adopted for the formation factor enables us to extend it to partially saturated system, following the approach of *Perkins et al.* [1956]. The apparent formation factor for a partially saturated porous system, $F_f(S_w)$, is related to porosity, fluid tortuosity τ_f, and saturation S_w,

$$F_f(S_w) = \frac{\tau_f^{\,2}}{\phi S_w} \tag{6}$$

Generally, the relationship between tortuosity in partially saturated condition τ_f and tortuosity in fully saturated condition τ_p has been explored extensively in the literature, as described by *Ghanbarian et al.* [2013]; *Jougnot et al.* [2018], and two tortuosities are related by $\tau_f \geq \tau_p$. The resistivity index I from Equation (1) can be expressed as a function of the formation factor ratio between equations (5) and (6), as shown below [*Perkins et al.*, 1956],

$$I = \frac{F_f\left(S_w\right)}{F} = \frac{\left(\frac{\tau_f}{\tau_p}\right)^{\eta}}{S_w} \tag{7}$$

Theoretically, $\eta = 2$ for three-dimensional space [*Cai et al.*, 2017]. However, the value of the exponent index η in the ratio τ_s/τ_p is uncertain. For instance, *Winsauer et al.* [1952] observed that η was 1.67 in their experimental data. Therefore, we use $T(S_w)$ instead of $\left(\tau_f/\tau_p\right)^{\eta}$ in Equation (7) to eliminate the influence of η. As a result, the expression for I transforms to,

$$I = \frac{T\left(S_w\right)}{S_w} \tag{8}$$

The uncertain relation between the capillary diameter of conducting phase r and the scaling factor λ complicates the determination of tortuosity [*Fu et al.*, 2021]. Therefore, the current path in saturated space is considered a 'straight-line' reference for the current path in partially saturated media, resulting in the calculation of relative tortuosity $T(S_w)$. Assuming a linear relationship between the length L_0 and the maximum pore diameter $r_{\max}$ of porous media, with the ratio represented by α, as

$$L_0 = \alpha r_{\max} \tag{9}$$

and the scaling λ in Equation (3) has the same linear correlation with fluid capillary diameter r in the pore,

$$\lambda = \alpha r \tag{10}$$

Then, substituting equations (9) and (10) to Equation (3), the relative tortuosity $T(S_w)$ becomes,

$$T\left(S_w\right) = \left(\frac{r_{\max}}{r}\right)^{D_{Tf}-1} \tag{11}$$

where D_{Tf} is the tortuosity fractal dimension in the partially saturated media. Combining equations (4) and (11), and selecting $\theta = \phi S_w$, we can obtain the expression,

$$T\left(S_w\right) = S_w^{\frac{D_{Tf}-1}{D_F - D_E}} \tag{12}$$

where D_E is the Euclidean dimension of the embedding space ($D_E = 2$ and 3 in two-

and three-dimensional space, respectively). Combining equations (8) and (12), the resistivity index can be expressed as,

$$I = \frac{T\left(S_w\right)}{S_w} = S_w^{-\frac{D_{Tf}-1}{D_E-D_F}-1} \tag{13}$$

The experimental saturation exponent in Equation (1) can be reformulated as a fractal-based expression derived from Equation (13),

$$n = \frac{D_{Tf}-1}{D_E-D_F}+1 \tag{14}$$

The expression of n is similar to that of the cementation m, as derived from previous work [*Wei et al.*, 2015]. However, tortuosity differs between saturated and unsaturated pore spaces. The distinction primarily results from the tortuosity fractal dimension, where the ion flow path in the partially saturated pores is longer than that in fully saturated pores [*Saomoto and Katagiri*, 2015], leading to $D_{Tf} \geq D_{Tp}$. Nonetheless, the randomness of the current path in partially saturated pore space may give rise to $D_{Tf} < D_{Tp}$.

Thus, an Archie-like electrical conductivity model with three empirical parameters takes the following form [*Winsauer et al.*, 1952; *Balberg*, 1986],

$$\sigma = a\sigma_w \phi^m S_w^n \tag{15}$$

where σ_w is the electrical conductivity of the fluid phase. The empirical parameters a and m were assigned physical meaning based on fractal geometry [*Wei et al.*, 2015],

$$m = \frac{D_{Tp}-1}{D_E-D_F}+1 \tag{16}$$

$$a = \frac{D_F + D_{Tp} - 1}{D_F} \tag{17}$$

In Equation (17), as porosity approaches 100%, D_{Tp} tends to 1, implying that a will also approach 1. This behaviour ensures that, in the high-porosity limit, the model correctly predicts the electrical conductivity to converge toward that of the saturating brine. The exponent m is known as the cementation exponent in Archie's first equation for full saturation. When comparing equations (14) and (16), m and n take similar forms,

differing only in their respective tortuosity fractal dimensions. The saturation exponent n is related to the tortuosity fractal dimension in partially saturated porous media, D_{Tf}.

Previous studies [*Guarracino et al.*, 2014; *Thanh et al.*, 2020; *Soldi et al.*, 2024] have shown that one way to handle different fractal dimensions for fully and partially saturated states is to characterize the pore fractal dimension and then predict how tortuosity evolves as saturation changes based on which pore sizes remain filled by means of Laplace equation. However, D_{Tf} cannot be precisely expressed by a mathematical function or an effective empirical model. In Equation (14), the critical factor is the difference between fractal dimensions of fully saturated and partially saturated rock. It is an impossible task to obtain these fractal parameters for different saturation states.

2.2 Calculation of fractal dimensions

We now attempt to derive a modified Archie equation that utilizes the fractal dimensions of fully saturated porous media to predict electrical conductivity without the need to know the exact saturation state.

The apparent formation factor in the modified Archie equation can be expressed in following form using an exponent m_1,

$$F = a\phi^{-m} = \phi^{-\left(m-\frac{\log a}{\log \phi}\right)} = \phi^{-m_1} \tag{18}$$

Equation (18) represents the standard Archie equation, and its form is similar to that of the resistivity index. The relationship between m and n is complex, and calculating either parameter individually is challenging. If the cementation factor m_1 represents a combination of m and n, as introduced by *Gkortsas et al.* [2018], then the electrical conductivity model can express the following form,

$$\sigma = \sigma_w \left(\phi S_w\right)^{m_n} \tag{19}$$

Note that m_n is an approximate parameter representing the exponent relationship between ϕ and S_w. In the special case where $m_n = m = n$, Equation (19) reverts to the standard Archie equation, $\sigma = \sigma_w \phi^m S_w^n$. By comparing Equation (16) through (19), we derive an expression for m_n as following,

$$m_n = \frac{D_{Tp} - 1}{D_E - D_F} - \frac{\ln \dfrac{D_F + D_{Tp} - 1}{D_F}}{\ln \phi} + 1 \tag{20}$$

Equation (20) presents a simplified equation that applies the fractal dimensions of fully saturated porous media to describe the transition from partially saturated to fully saturated conditions. In the case of D_{Tp}, a method for obtaining its value is introduced in the next chapter. The origin model, which combined Archie equation with the *Winsauer et al.* [1952] modification which is given as Equation (15), contains three parameters, making it more complex than Archie equation for full saturation (one parameter in its original form [*Archie*, 1942] and 2 in *Winsauer et al.* [1952] modified version. In contrast, the unified model (Equation (19)) involves only two parameters (m and n or D_{Tp} and D_F).

This new method is simple but effective for predicting the resistivity of partially saturated rock based on measured fractal dimensions. In fact, calculating fractal dimensions separately for fully saturated and partially saturated media may reduce accuracy. Moreover, it is often impossible to obtain all the necessary fractal parameters.

A key problem lies in the difference between the fractal dimensions of fully saturation and partial saturation. While the fractal dimensions for fully saturated porous media can be measured experimentally, observing the instantaneous saturation process is highly complex, which complicates the calculation of fractal dimensions. As a result, fractal dimensions for the drainage or imbibition process are often unavailable. Therefore, predicting fractal dimensions based on existing data becomes necessary.

Compared to the classical Archie-like equation (Equation (15)) or its modified version and the previous published models, the proposed model offers better performance in predicting electrical conductivity. One advantage is the clearer physical interpretation of the empirical parameters m and n. When the pore fractal dimension is known, the proposed model is capable of predicting values within a small error margin, as we show below.

3. Comparing the model with experimental data

Two different types of rock data are applied to validate the presented model, (i) data with known pore fractal dimension, and (ii) data with unknown pore fractal dimension.

Data from two types of sandstone samples, 'Data1' from *Li and Williams* [2007] and 'Data2' from *Chen et al.* [2023] have been used (see Table 1). These two data sets both have known pore fractal dimension, allowing for easy calculation of the tortuosity fractal dimension.

Two additional data sets,'Data3' from *Siddiqui* [2007] and 'Data4' from *Al-Gathe* [2009] (also listed in Table 1), include grainstone, packstone and wackestone samples. These data sets lack measured fractal dimensions, requiring the fractal dimensions to be estimated based on porosity and formation factor.

The basic structural and transport parameters are provided in Table 1. The narrow range of porosity is associated with a wide variation in physical properties, which leads to inaccurate predictions with Archie-like equation. The ratio of formation factor between the maximum and minimum values reaches a factor of 45, complicating predictions made by both the newly presented model and the Archie-like equation. It is important to note that the pore fractal dimension in Data1 and Data2 fall within significantly different ranges, above 2 for Data1, and below 2 for Data2. This difference is due to the type of fractal object, which was measured to provide the D_{Tp}; Data1 measured surface roughness in a volume, while Data2 calculates it from boundaries in binary images from the thin sections. Consequently, intercomparison is clearer by calculating the appropriate Hausdorff number H_{Tp} (i.e., the dimensionality by which a fractal dimension exceeds its Euclidean dimension), which is also included in Table 1.

3.1 Calculation of fractal dimensions

Data sets Data3 and Data4 both lack a measured pore fractal dimension. Data3 (from *Siddiqui* [2007]) includes 16 core samples and Data4 (from *Al-Gathe* [2009]) includes 44 core samples. In general, determining the value of D_F experimentally requires significant time, as methods such as scanning electron microscopy [*Kong et al.*, 2019] or nuclear magnetic resonance [*Ouyang et al.*, 2016] are typically used. Moreover, no

universally accepted method exists to validate the precision of D_F. A standard method for estimating D_F has been tested by *Liu et al.* [2019] and *Song et al.* [2019],

$$D_F = D_E - \frac{\ln \phi}{\ln \frac{\lambda_{\min}}{\lambda_{\max}}} \tag{21}$$

The value of $\lambda_{min}/\lambda_{max}$ is typical determined by fitting the pore fractal dimension and porosity from samples. In Figure 2, the fitting curve using $\lambda_{min}/\lambda_{max} = 0.005$ shows good agreement, making this value applicable for the current study.

The tortuosity fractal dimension can be estimated using porosity, the formation factor and the pore fractal dimension. These fractal dimensions are derived from measurements and calculations performed on fully saturated rock. It should be noted that the influence of surface conduction is ignored in this estimation. From the discussion in *Wei et al.* [2015] work, D_{Tp} can be expressed as,

$$D_{Tp} = \left(D_E - D_F + 1\right) + \left(D_E - D_F\right)\frac{\ln D_F - \ln\left(D_E F \phi^2\right)}{\ln \phi} \tag{22}$$

An obvious drawback of this equation is that D_{Tp} depends only on the formation factor F, D_F, and ϕ, rather than on S_w as in Equation (14). This implies that the tortuosity fractal dimension of partially saturated rock cannot be predicted directly. Nevertheless, based on the definition of tortuosity fractal dimension [*Wheatcraft and Tyler*, 1988], a reasonable assumption can be made. The degree of complexity in tortuosity may remain stable as the fluid-filling space transitions to the pore space (or as λ decreases in Equation (3)) during the shift from fully saturated to unsaturated conditions. In other words, the tortuosity fractal dimension may be regarded as constant, independent of the level of saturation.

3.2 Estimation for the model of Equation (19)

In the newly presented model, equations (19) and (20) are applied to estimate D_{Tp} and D_F from the data shown in Table 1. Once the pore fractal dimension is obtained, the tortuosity fractal dimension is calculated using Equation (22). The results of calculating m_n using Equation (20) to predict electrical conductivity as shown in Figure 3. A

comparison with the Archie-like combined equation (Equation (15)), where m is calculated from the formation factor and porosity, and n from resistivity index and saturation, is also displayed in Figure 3. The Root Mean Square Error (RMSE) is used as a quantitative measure to evaluate the results.

Figure 3 shows, expectedly, that the new model with known pore fractal dimension (figure parts a and b) exhibits lower RMSE values (3.16% and 1.23%, respectively) than those with unknown pore fractal dimension (parts c and d) at 9.11% and 11.06%, respectively. Datasets where the fractal dimension is unknown (Data3 and Data4) do not provide precise predictions of electrical conductivity. In these cases, the data are more scattered compared to when the fractal dimension is known. This suggests that accurate determination of fractal dimensions is crucial for estimating the electrical conductivity of porous media.

Overall, the maximum RMSE from the new model (Figure 3) is relatively low, at 11.06%, indicating that the model can reliably predict data with an RMSE of less than 15%. In all cases the fit (low RMSEs) is significantly better than the performance of the conventional Archie law approach (Equation (15)) when using the new model. The conventional Archie's approach provides RMSEs in the range between 15% and 25% in all cases except Data2, where the fit is remarkably good (RMSE = 1.63%). This case (Figure 3b) is particularly pertinent because the co-linearity of the new model fit with the good conventional Archie's law fit represents a cross-validation of both methods for this particular dataset.

The primary focus of this work is the application of predicting saturation from electrical conductivity data. The estimation of various saturation levels, obtained by reversing Equation (19), is shown in Figure 4. This highlights the distinction between the presented model and Archie-like model. The fitting line $y = 0.07 + 1.045x$ (coefficient of determination, R^2=0.951) from the presented model is closer to the line $y = x$, compared to the result from the conventional Archie equation ($y = 0.031 + 1.275x$, R^2=0.831). It should be noted that the new model has a gradient only slightly greater than unity and a small offset, while the conventional Archie model has not only a greater offset, but a significantly deviant gradient.

The 95% predicted band, which indicates each model's uncertainty by representing the range within which we expect 95% of future data points to fall is much smaller for the new model (Figure 4a) than the conventional Archie's model (Figure 4b), indicating the former's higher accuracy.

A number of scattered data points exceed the boundary of the 95% predicted band in Figure 4. In the predictions from the new model, these deviations mainly arise from Data4. However, the conventional Archie equation results in a greater deviation, with the fitting line $y = 0.031 + 1.275x$ deviating significantly from the 1:1 line, not just as an offset, but also with a change in gradient. This leads to inaccurate estimates for Data1, Data2 and Data4. The results of predicting electrical conductivity and saturation demonstrate that the new model performs better than the conventional combined Archie equation.

Similar to other approaches in the literature, *Soldi et al.* [2024] proposed a model based on a bundle of tortuous capillary tubes, each having periodic radius variations and a fractal distribution of pore sizes. Their results indicate that this model outperforms the one proposed by *Thanh et al.* [2020]. In this work, we compare our model's performance to that of *Soldi et al.* [2024] using the same experimental dataset originally published by *Saafan et al.* [2023]. As shown in Table 2, our model achieves a lower RMSE and thus provides superior predictive capabilities under these test conditions.

4. The relationship between fractal and Archie parameters

An interesting relationship exists between the Archie's parameters and the fractal dimensions within the condition of partial saturation, which warrants further discussion. In equations (14) and (16), the cementation exponent *m* and the saturation exponent *n* share the same mathematical form (as foreseen by [*Glover*, 2010]. If the tortuosity dimensions are similar ($D_{Tf} \approx D_{Tp}$), the cementation exponent and saturation exponent are also expected to be similar. However, *m* and *n* differ in most reservoir rocks, which suggests $D_{Tp} \neq D_{Tf}$. The irregular variation observed in Figure 5(b), makes it challenging to establish a direct correlation between *m* and *n*.

The new model employs multiple fractal dimensions to describe the behaviour of

partially saturated porous media. From the view of principle of Occam's razor, simpler models should be preferred when they provide an adequate description. The inclusion of these parameters is intended to capture the subtle behaviour of fluid distribution and electrical conductivity. We will acknowledge that future work should explore whether a more effective model could yield similar predictive power without sacrificing accuracy.

Furthermore, establishing an effective bound to limit the range of electrical conductivity can help improve the accuracy of logging. It is important to assess whether the new model can define reliably both upper and lower boundaries, and to characterize the influence of fractal dimensions on electrical conductivity in partially saturated rock. These issues are discussed in the following sub-sections.

4.1 The relationship between *m* and *n*

In the past, several common microstructural characteristics of rocks [*Cai et al.*, 2019], such as pore-throat structure, connectivity, and tortuosity, have been used to calculate the bulk electrical conductivity of a rock. However, these factors are often insufficient to fully quantify the relationship between porosity and electrical conductivity, and additional challenges exist in accurately quantifying electrical conductivity. One such challenge is the ambiguous relationship between cementation exponent and saturation exponent in the conventional Archie model. Significantly, the exponent n is not only related to the saturation but is also dependent on the distribution of pores and fluids (i.e., their connectedness). In Equation (15), m and n share the same format, except for difference in tortuosity fractal dimensions. This suggests that the common influencing factors of m and n are the amount and connectedness of the conducting phase. Such ideas are already formulated theoretically in the Generalized Archie's Law for n-phases [*Glover*, 2010].

To clarify this relationship between m and n, D_{Tf} can be determined using n using Equation (14), and D_{Tp} is calculated from m from Equation (16) for fully saturated porous media. Therefore, the relationship assuming D_F remains stable during the drainage or imbibition process, and can be expressed as follows,

$$m - n \propto D_{Tp} - D_{Tf} \tag{23}$$

In Equation (23), if $D_{Tf} \approx D_{Tp}$, this indicates that m and n are also approximately equal. A similar conclusion can be found in *Glover* [2010], where if the pore phase is dissolved, discounted, or removed by the fluid phase, such as when ϕ is converted to S_w, the exponents m and n could replace each other.

To evaluate the relationship between two exponents, m is calculated using the data on the formation factor and porosity, while n is computed by fitting resistivity index and saturation. The variations in $D_{Tf} \approx D_{Tp}$ and $m - n$ with saturation are depicted in Figure 5. The results indicate that the fluctuations in $D_{Tf} \approx D_{Tp}$ mostly fall within a $\pm 10\%$ error range, as seen in Figure 5(a). However, most values of $m - n$ lie outside the -10% to 10% range, as shown in Figure 5(b), indicating the relationship between two exponents, $m - n \approx 0$, does not hold in these datasets.

Fortunately, following the analysis of m, n and m_n by *Gkortsas et al.* [2018], we find an analogous expression based on Equation (14) in their study, reformulating the relationship as follows,

$$m_n \propto \beta(m - n) + n \tag{24}$$

and

$$\beta = \frac{1}{N}\sum_{i=1}^{N} \frac{\ln \phi}{\ln \phi + \ln\left[S_w(i)\right]},$$

where N denotes the total number of saturation measurements for a core. In Equation (24), this symbol '$\propto$' indicates that the two sides correspond to different computational approaches, where m_n is calculated using Equation (20), while m is estimated based on formation factor and porosity measurements, and n is derived from regression analysis of resistivity index and saturation data. Therefore, this relation cannot be directly employed to determine n.

We compare the estimated m_n from Equation (20) with its theoretical value, $\beta(m - n) + n$, in Figure 6, showing that the predicted m_n aligns reasonably well with the theoretical model. This suggests that the relationship between m and n is valid for these datasets. Furthermore, this distinct correlation enhances the investigation of transport properties through electrical characteristics, as explored in previous works

[*Doussan and Ruy*, 2009; *Saafan et al.*, 2023].

4.2 Unpredictable behaviour of the resistivity index and its bounds model

Accurately determining the tortuosity fractal dimension is nearly impossible with limited pore structure and fluid distribution data. Saturation depends on the fluid distribution within the pore during the displacement process, which is influenced by both hysteresis and the electrical resistivity jump phenomenon during imbibition and drainage [*Knight*, 1991; *Mawer et al.*, 2015; *Umezawa et al.*, 2021]. These processes often result in unstable fluid distributions. While the overall characteristics of the fluid geometries can be reproduced, the fluid will not occupy identical locations in repeated experiments [*Knight*, 1991]. When fluids are randomly distributed in pore space at medium saturation, and a water film forms on some grain surface, the surface conductivity will affect the prediction of the resistivity index [*Maineult et al.*, 2018; *Mustofa et al.*, 2022]. During the displacement stage, connected fluid can form different flow paths, leading to variations in tortuosity. According to Equation (7), the resistivity index is a function of tortuosity, meaning that random flow paths can cause fluctuations in the resistivity index.

Rock structural imaging technology, such as computed tomography and nuclear magnetic resonance, can explicitly analyse flow paths when combined with numerical simulation methods [*Xia et al.*, 2019], but these techniques are time-consuming. For most rock samples, precise determination of tortuosity is limited by the availability of microstructural data. One method for estimating the range of resistivity index is by determining its boundaries. It is widely recognized that the minimal tortuosity dimension is 1. If $D_{Tf} \approx D_{Tp}$ is applied to obtain the average of the resistivity index, then the minimal resistivity index (I_{min}) and maximal resistivity index (I_{max}) can be expressed as,

$$\begin{aligned} I_{\min} &= S_w^{-1} \\ I_{\max} &= 2I - I_{\min} = 2S_w^{-\frac{D_{Tp}-1}{D_E-D_F}-1} - S_w^{-1} \end{aligned} \tag{25}$$

Equation (25) represents the lower and upper boundaries for the resistivity index

as a function of saturation.

Figure 8 shows an example of the bounds model. This indicates that the use of the tortuosity fractal dimension could better constrain the range of the resistivity index. The bounds model in Equation (25) helps explain the deviation in Equation (23) caused by the uncertainty of the tortuosity fractal dimension in partially saturated rock. Moreover, the performance of the proposed bounds model (Equation (25)) is evaluated by comparing it with other bounds models [*Cai et al.*, 2017], including the parallel, the perpendicular, the random models. These comparisons also include the Hashin-Shtrikman (H-S) upper and lower bounds, the Waff model and the modified brick-layer model. As the illustration in Figure 7, the proposed bounds model effectively constrains the predicted range of electrical conductivity.

In most sedimentary rocks, the distribution of saturation affects both tortuosity and resistivity, particularly due to clay minerals and water blockage, with the conducting fluid being the wetting phase in the rock system comprised of solids, pores and brine. If the relationship $D_{Tf} \approx D_{Tp}$ represents the normal tortuosity condition, water blockage could result in a different flow path within the pore space (Figure 8). For example, external conditions may alter the saturation distribution, changing the tortuosity. As a result, the presented model may overestimate (Figure 8(a)) or underestimate (Figure 8(c)) the resistivity index. However, the goal is to develop a more precise model of the resistivity index by incorporating pore structure parameters from available experimental data.

5. Conclusion

This paper describes the development of an analytical model to predict electrical conductivity in partially saturated porous media with a solid insulator matrix based on the Pore-Solid Fractal model. The model considers the effect of tortuosity as a function of saturation and microstructural parameters, including pore fractal dimension, and the tortuosity fractal dimension of porous media. To reduce the influence of unmeasurable fractal parameters, we propose a method to combine these fractal dimensions. Available experimental data were used to test the effectiveness of the proposed model. The

theoretical calculations aligned well with the experimental results. The assumed theoretical relationship between the cementation exponent and the resistivity index, $m \approx n$, does not hold universally across the dataset. Instead, an alternative expression based on *Gkortsas et al.* [2018] can enhance the practical application of the conventional combined Archie equation, exhibiting good agreement with measurements. Finally, a bounds equation is presented as an alternative for an accurate tortuosity fractal dimension in cases where fluid distribution information is insufficient.

This study focused on partially saturated, isotropic, and three-phase (fluid, pores, and solids) porous media, where pore size distributions follow a fractal scaling law. Future research should extend the developed model to non-fractal porous media and non-insulated solid phases, such as those involving mineral conduction at high temperatures or the presence of partial melting. Additionally, models should consider non-insulating interfaces between water and minerals, such as involving surface conduction.

Acknowledgments

The authors acknowledge the valuable discussions with Dr. Xiaojun Chen. This work is supported by the National Natural Science Foundation of China (Nos. 42104073, 42004086, 42172159). Additional funding is provided by the Fundamental Research Funds for the Central Universities, China University of Geosciences (Wuhan) (Nos. CUG2106339 and CUGGC04) and the China Scholarship Council.

Data and materials availability

Data associated with this research are available and can be accessed via the following URL: https://doi.org/10.5281/zenodo.13981500.

References

Al-Gathe, A. (2009), Analysis of Archie's parameters determination techniques, King Fahd University of Petroleum and Minerals.

Archie, G. E. (1942), The electrical resistivity log as an aid in determining some reservoir characteristics, *Transactions of the AIME*, *146*(01), 54-62, doi:10.2118/942054-g.

Balberg, I. I. (1986), Excluded-volume explanation of Archie's law, *Physical Review B*, *33*(5), 3618-3620, doi:10.1103/PhysRevB.33.3618.

Bird, N. R. A., E. Perrier, and M. Rieu (2000), The water retention function for a model of soil structure with pore and solid fractal distributions, *Eur. J. Soil Sci.*, *51*(1), 55-63, doi:10.1046/j.1365-2389.2000.00278.x.

Cai, J. C., W. Wei, X. Y. Hu, and D. A. Wood (2017), Electrical conductivity models in saturated porous media: A review, *Earth-Sci. Rev.*, *171*, 419-433, doi:10.1016/j.earscirev.2017.06.013.

Cai, J. C., Z. Zhang, W. Wei, D. M. Guo, S. Li, and P. Q. Zhao (2019), The critical factors for permeability-formation factor relation in reservoir rocks: Pore-throat ratio, tortuosity and connectivity, *Energy*, *188*, 116051, doi:10.1016/j.energy.2019.116051.

Chen, X., L. D. Thanh, C. Luo, P. Tahmasebi, and J. Cai (2023), Dependence of electrical conduction on pore structure in reservoir rocks from the Beibuwan and Pearl River Mouth Basins: A theoretical and experimental study, *Geophysics*, *88*(2), MR35-MR53, doi:10.1190/geo2021-0682.1.

Coleman, S. W., and J. C. Vassilicos (2008), Tortuosity of unsaturated porous fractal materials, *Phys. Rev. D*, *78*(1), 016308, doi:10.1103/PhysRevE.78.016308.

Doussan, C., and S. Ruy (2009), Prediction of unsaturated soil hydraulic conductivity with electrical conductivity, *Water Resour. Res.*, *45*(10), doi:10.1029/2008WR007309.

Duy Thanh, L., D. Jougnot, P. Van Do, and N. Van Nghia A (2019), A physically based model for the electrical conductivity of water-saturated porous media, *Geophys. J. Int.*, *219*(2), 866-876, doi:10.1093/gji/ggz328.

Friedman, S. P., and N. A. Seaton (1998), Critical path analysis of the relationship between permeability and electrical conductivity of three-dimensional pore networks, *Water Resour. Res.*, *34*(7), 1703-1710, doi:10.1029/98WR00939.

Fu, J., H. R. Thomas, and C. Li (2021), Tortuosity of porous media: Image analysis and physical simulation, *Earth-Sci. Rev.*, *212*, 103439, doi:10.1016/j.earscirev.2020.103439.

Garing, C., L. Luquot, P. A. Pezard, and P. Gouze (2014), Electrical and flow properties of highly heterogeneous carbonate rocks, *AAPG Bull.*, *98*(1), 49-66, doi:10.1306/05221312134.

Ghanbarian-Alavijeh, B., and A. G. Hunt (2012), Unsaturated hydraulic conductivity in porous media: Percolation theory, *Geoderma*, *187–188*, 77-84, doi:10.1016/j.geoderma.2012.04.007.

Ghanbarian, B., A. G. Hunt, R. P. Ewing, and M. Sahimi (2013), Tortuosity in porous media: A critical review, *Soil Sci. Soc. Am. J.*, *77*(5), 1461-1477, doi:10.2136/sssaj2012.0435.

Ghanbarian, B., and M. Sahimi (2017), Electrical Conductivity of Partially Saturated Packings of Particles, *Transp. Porous Media*, *118*(1), 1-16, doi:10.1007/s11242-017-0821-4.

Gkortsas, V.-M., L. Venkataramanan, K. Fellah, D. Ramsdell, C.-Y. Hou, and N. Seleznev (2018), Comparison of different dielectric models to calculate water saturation and estimate textural parameters in partially saturated cores, *Geophysics*, *83*(5), E303-E318, doi:10.1190/geo2018-0100.1.

Glover, P. W. J. (2010), A generalized Archie's law for n phases, *Geophysics*, *75*(6), E247-E265, doi:10.1190/1.3509781.

Glover, P. W. J. (2015), Geophysical properties of the near surface earth: Electrical properties, in *Treatise on geophysics: Second edition*, edited by G. Schubert, pp. 89-137, Elsevier, Netherlands, doi:10.1016/B978-0-444-53802-4.00189-5.

Glover, P. W. J. (2016), Archie's law – a reappraisal, *Solid Earth*, *7*(4), 1157-1169, doi:10.5194/se-7-1157-2016.

Glover, P. W. J. (2017), A new theoretical interpretation of Archie's saturation exponent,

Solid Earth, *8*(4), 805-816, doi:10.5194/se-8-805-2017.

Glover, P. W. J., M. J. Hole, and J. Pous (2000), A modified Archie's law for two conducting phases, *Earth Planet. Sci. Lett.*, *180*(3-4), 369-383, doi:10.1016/S0012-821X(00)00168-0.

Greve, A. K., H. Roshan, B. F. J. Kelly, and R. I. Acworth (2013), Electrical conductivity of partially saturated porous media containing clay: An improved formulation, *J. Geophys. Res.*, *118*(7), 3297-3303, doi:10.1002/jgrb.50270.

Guarracino, L., T. Rötting, and J. Carrera (2014), A fractal model to describe the evolution of multiphase flow properties during mineral dissolution, *Adv. Water Resour.*, *67*, 78-86, doi:10.1016/j.advwatres.2014.02.011.

Hamamoto, S., P. Moldrup, K. Kawamoto, and T. Komatsu (2010), Excluded-volume expansion of Archie's law for gas and solute diffusivities and electrical and thermal conductivities in variably saturated porous media, *Water Resour. Res.*, *46*(6), doi:10.1029/2009WR008424.

Hunt, A. G., R. P. Ewing, and B. Ghanbarian (2014), *Percolation theory for flow in porous media*, 3rd ed., Springer, Berlin.

Jougnot, D., J. Jiménez-Martínez, R. Legendre, T. Le Borgne, Y. Méheust, and N. Linde (2018), Impact of small-scale saline tracer heterogeneity on electrical resistivity monitoring in fully and partially saturated porous media: Insights from geoelectrical milli-fluidic experiments, *Adv. Water Resour.*, *113*, 295-309, doi:10.1016/j.advwatres.2018.01.014.

Jougnot, D., A. Revil, and P. Leroy (2009), Diffusion of ionic tracers in the Callovo-Oxfordian clay-rock using the Donnan equilibrium model and the formation factor, *Geochim. Cosmochim. Acta*, *73*(10), 2712-2726, doi:10.1016/j.gca.2009.01.035.

Knight, R. (1991), Hysteresis in the electrical resistivity of partially saturated sandstones, *Geophysics*, *56*(12), 2139-2147, doi:10.1190/1.1443028.

Kong, L., M. Ostadhassan, X. Hou, M. Mann, and C. Li (2019), Microstructure characteristics and fractal analysis of 3D-printed sandstone using micro-CT and SEM-EDS, *J. Pet. Sci. Eng.*, *175*, 1039-1048, doi:10.1016/j.petrol.2019.01.050.

Li, K., B. Hou, H. Bian, H. Liu, C. Wang, and R. Xie (2019), Verification of model for

calculating capillary pressure from resistivity using experimental data, *Fuel*, *252*, 281-294, doi:10.1016/j.fuel.2019.04.083.

Li, K., and W. Williams (2007), Determination of capillary pressure function from resistivity data, *Transp. Porous Media*, *67*(1), 1-15, doi:10.1007/s11242-006-0009-9.

Liu, L., S. Dai, F. Ning, J. Cai, C. Liu, and N. Wu (2019), Fractal characteristics of unsaturated sands − implications to relative permeability in hydrate-bearing sediments, *J. Nat. Gas Sci. Eng.*, *66*, 11-17, doi:10.1016/j.jngse.2019.03.019.

Maineult, A., D. Jougnot, and A. Revil (2018), Variations of petrophysical properties and spectral induced polarization in response to drainage and imbibition: a study on a correlated random tube network, *Geophys. J. Int.*, *212*(2), 1398-1411, doi:10.1093/gji/ggx474.

Mawer, C., R. Knight, and P. K. Kitanidis (2015), Relating relative hydraulic and electrical conductivity in the unsaturated zone, *Water Resour. Res.*, *51*(1), 599-618, doi:10.1002/2014wr015658.

Mohamad, A. M., and G. M. Hamada (2017), Determination techniques of Archie's parameters: a, m and n in heterogeneous reservoirs, *J. Geophys. Eng.*, *14*(6), 1358-1367, doi:10.1088/1742-2140/aa805c.

Mustofa, M. B., U. Fauzi, F. D. E. Latief, and W. Warsa (2022), Experimental and modeling of electrical resistivity changes due to micro-spatial distribution of fluid for unconsolidated sand, *J. Pet. Sci. Eng.*, *208*, 109472, doi:10.1016/j.petrol.2021.109472.

Niu, Q., and C. Zhang (2018), Physical explanation of Archie's porosity exponent in granular materials: A process-based, pore-scale numerical study, *Geophys. Res. Lett.*, *45*(4), 1870-1877, doi:10.1002/2017gl076751.

Niu, Q., and C. Zhang (2019), Permeability prediction in rocks experiencing mineral precipitation and dissolution: A numerical study, *Water Resour. Res.*, *55*(4), 3107-3121, doi:10.1029/2018wr024174.

Norbisrath, J. H., G. P. Eberli, B. Laurich, G. Desbois, R. J. Weger, and J. L. Urai (2015), Electrical and fluid flow properties of carbonate microporosity types from

multiscale digital image analysis and mercury injection, *AAPG Bull.*, *99*(11), 2077-2098, doi:10.1306/07061514205.

Ojeda, G., E. Perfect, J. M. Alcañiz, and O. Ortiz (2006), Fractal analysis of soil water hysteresis as influenced by sewage sludge application, *Geoderma*, *134*(3), 386-401, doi:10.1016/j.geoderma.2006.03.011.

Ouyang, Z., D. Liu, Y. Cai, and Y. Yao (2016), Fractal analysis on heterogeneity of pore–fractures in middle–high rank coals with NMR, *Energy Fuels*, *30*(7), 5449-5458, doi:10.1021/acs.energyfuels.6b00563.

Peng, R., B. Di, P. W. J. Glover, J. Wei, P. Lorinczi, P. Ding, Z. Liu, Y. Zhang, and M. Wu (2019), The effect of rock permeability and porosity on seismoelectric conversion: experiment and analytical modelling, *Geophys. J. Int.*, *219*(1), 328-345, doi:10.1093/gji/ggz249.

Perkins, F. M., J. S. Osoba, and K. H. Ribe (1956), Resistivity of sandstones as related to the geometry of their interstitial water, *Geophysics*, *21*(4), 1071-1084, doi:10.1190/1.1438302.

Perrier, E., N. Bird, and M. Rieu (1999), Generalizing the fractal model of soil structure: the pore–solid fractal approach, *Geoderma*, *88*(3–4), 137-164, doi:10.1016/S0016-7061(98)00102-5.

Rashid, F., P. W. J. Glover, P. Lorinczi, D. Hussein, R. Collier, and J. Lawrence (2015), Permeability prediction in tight carbonate rocks using capillary pressure measurements, *Mar. Pet. Geol.*, *68*, 536-550, doi:10.1016/j.marpetgeo.2015.10.005.

Rembert, F., D. Jougnot, and L. Guarracino (2020), A fractal model for the electrical conductivity of water-saturated porous media during mineral precipitation-dissolution processes, *Adv. Water Resour.*, *145*, 103742, doi:10.1016/j.advwatres.2020.103742.

Revil, A. (2000), Thermal conductivity of unconsolidated sediments with geophysical applications, *J. Geophys. Res.*, *105*(B7), 16749-16768, doi:10.1029/2000JB900043.

Saafan, M., M. Mohyaldinn, and K. Elraies (2023), Obtaining capillary pressure curves

from resistivity measurements in low-permeability sandstone, *Geoenergy Science and Engineering*, *221*, 111297, doi:10.1016/j.petrol.2022.111297.

Saomoto, H., and J. Katagiri (2015), Direct comparison of hydraulic tortuosity and electric tortuosity based on finite element analysis, *Theor. Appl. Mech. Lett.*, *5*(5), 177-180, doi:10.1016/j.taml.2015.07.001.

Siddiqui, M. A. (2007), Investigation of the effect of heterogeneity on the resistivity of reservoir rock, M.S. thesis, 183 pp, King Fahd University of Petroleum and Minerals (Saudi Arabia), Ann Arbor.

Soldi, M., F. Rembert, L. Guarracino, and D. Jougnot (2024), Electrical conductivity model for reactive porous media under partially saturated conditions with hysteresis effects, *Adv. Water Resour.*, *193*, 104815, doi:10.1016/j.advwatres.2024.104815.

Song, W., D. Wang, J. Yao, Y. Li, H. Sun, Y. Yang, and L. Zhang (2019), Multiscale image-based fractal characteristic of shale pore structure with implication to accurate prediction of gas permeability, *Fuel*, *241*, 522-532, doi:10.1016/j.fuel.2018.12.062.

Thanh, L. D., D. Jougnot, P. Van Do, N. V. N. A, V. P. Tuyen, N. X. Ca, and N. T. Hien (2020), A physically based model for the electrical conductivity of partially saturated porous media, *Geophys. J. Int.*, *223*(2), 993-1006, doi:10.1093/gji/ggaa307.

Umezawa, R., M. Katsura, and S. Nakashima (2021), Effect of water saturation on the electrical conductivity of microporous silica glass, *Transp. Porous Media*, *138*(1), 225-243, doi:10.1007/s11242-021-01601-6.

Walker, E., and P. W. J. Glover (2018), Measurements of the Relationship Between Microstructure, pH, and the Streaming and Zeta Potentials of Sandstones, *Transp. Porous Media*, *121*(1), 183-206, doi:10.1007/s11242-017-0954-5.

Wang, H. T., and A. Revil (2020), Surface conduction model for fractal porous media, *Geophys. Res. Lett.*, *47*(10), e2020GL087553, doi:10.1029/2020gl087553.

Wang, Z., X. Li, H. Shi, W. Li, W. Yang, and Y. Qin (2020), Estimating the water characteristic curve for soil containing residual plastic film based on an improved

pore-size distribution, *Geoderma*, *370*, 114341, doi:10.1016/j.geoderma.2020.114341.

Wei, W., J. C. Cai, X. Y. Hu, and Q. Han (2015), An electrical conductivity model for fractal porous media, *Geophys. Res. Lett.*, *42*(12), 4833-4840, doi:10.1002/2015GL064460.

Wheatcraft, S. W., and S. W. Tyler (1988), An explanation of scale-dependent dispersivity in heterogeneous aquifers using concepts of fractal geometry, *Water Resour. Res.*, *24*(4), 566-578, doi:10.1029/WR024i004p00566.

Winsauer, W. O., J. H. M. Shearin, P. H. Masson, and M. Williams (1952), Resistivity of brine-saturated sands in relation to pore geometry, *AAPG Bull.*, *36*(2), 253-277, doi:10.1306/3D9343F4-16B1-11D7-8645000102C1865D.

Xia, Y., J. Cai, E. Perfect, W. Wei, Q. Zhang, and Q. Meng (2019), Fractal dimension, lacunarity and succolarity analyses on CT images of reservoir rocks for permeability prediction, *J. Hydrol.*, *579*, 124198, doi:10.1016/j.jhydrol.2019.124198.

Yue, W. Z., and G. Tao (2013), A new non-Archie model for pore structure: numerical experiments using digital rock models, *Geophys. J. Int.*, *195*(1), 282-291, doi:10.1093/Gji/Ggt231.

Table 1. Basic parameters for the four data sets.

Group	ϕ [-]	σ_w $[m/s]$	F [-]	Permeability $[mD]$	D_{Tp} [-]	H_{Tp} [-]	Source
Data1	0.077~0.321	3.25~12.82	8.0~380.9	0.02~3680.00	2.364~2.952	0.636~0.048	*Li and Williams* [2007]
Data2	0.104~0.192	4.09~14.36	26.9~124.8	0.09~17.80	1.570~1.684	0.43~0.316	*Chen et al.* [2023]
Data3	0.172~0.328	10.99	10.0~32.6	2.24~693.38	-	-	*Siddiqui* [2007]
Data4	0.100~0.260	11.11	4.9~222.4	0.39~613.05	-	-	*Al-Gathe* [2009]

Note: the value of D_{Tp} for Data3 and Data4 is unavailable.

Table 2. Comparison of RMSE between the *Soldi et al.* [2024] model and the proposed model.

Sample	RMSE (%) (*Soldi et al.* [2024] model)	RMSE (%) (This work)	Difference (%)
S6	5.01	1.60	-3.41
S9	2.58	0.90	-1.68
S13	2.88	0.63	-2.25
S14	1.19	0.42	-0.77
S16	1.97	1.28	-0.69
S18	1.17	0.77	-0.40

Note: Samples S6, S9, etc., match the naming used in *Soldi et al.* [2024]. A negative difference indicates lower RMSE for our model.

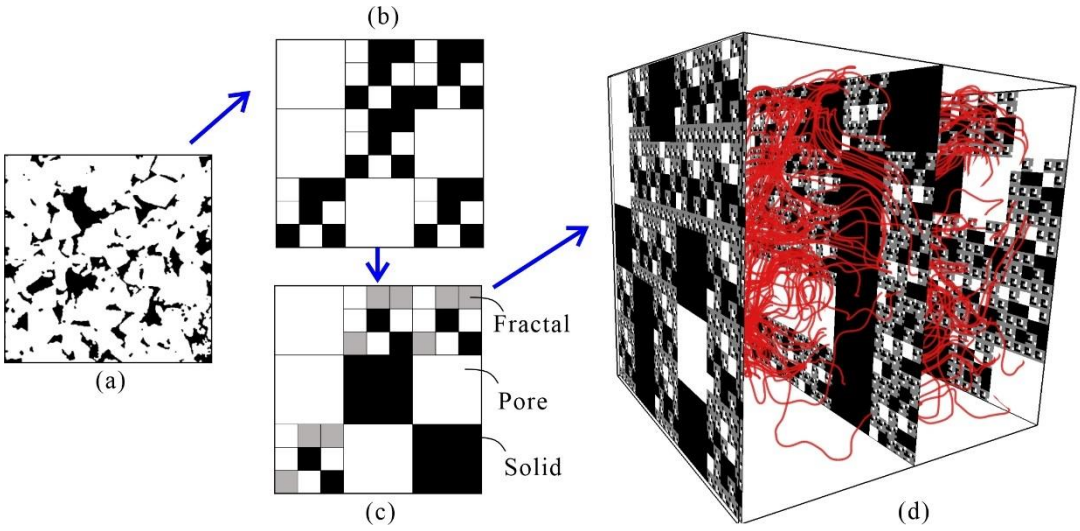

Figure 1. The process of transferring a rock structure into the Pore-Solid-Fractal (PSF) model and its fluid flow representation. (a) Two-dimensional binary image of rock structure, (b) Sierpinski carpet model, (c) PSF model. The grey region represents the fluid phase, while the remaining areas correspond to the non-fractal solid phase, and (d) streamtubes represented within the two-dimensional PSF model.

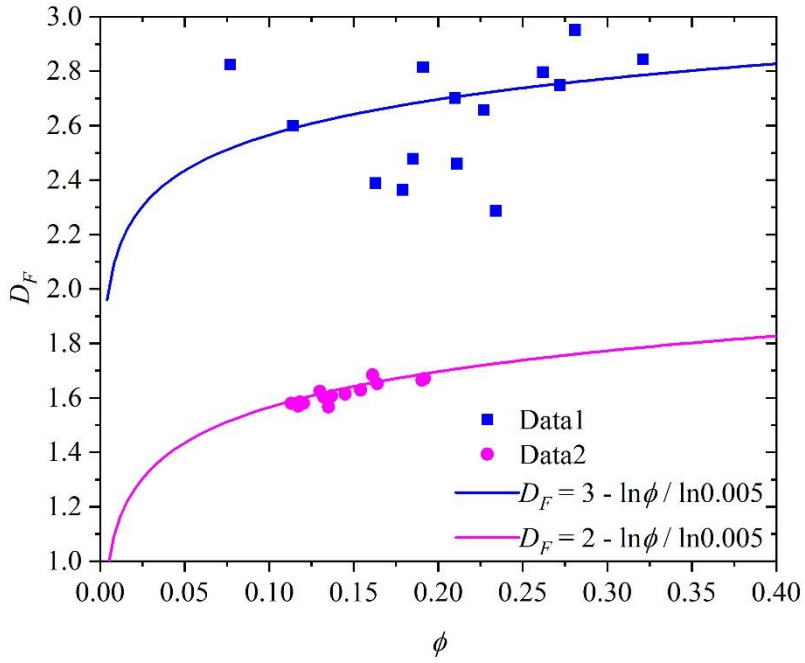

Figure 2. The relationship between pore fractal dimension and porosity in Equation (21), based on $\lambda_{min}/\lambda_{max} = 0.005$. Two different ranges of pore fractal dimension are shown, 2~3 for Data1 and 1~2 for Data2, using $D_E = 3$ and $D_E = 2$, respevtively.

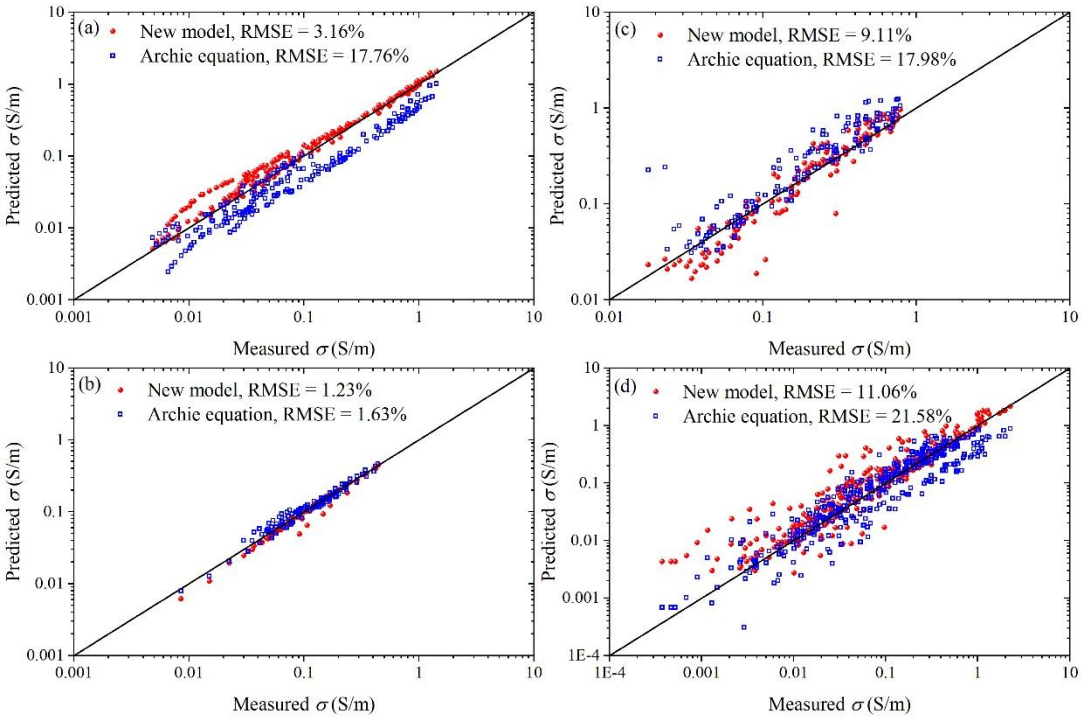

Figure 3. The prediction of electrical conductivity made using the model proposed in this work (Equation (19) and Equation (20)) and the conventional Archie's equation (Equation (15)) for (a) Data1, (b) Data2, (c) Data3, and (d) Data4. The black line represents the 1:1 line. Root Mean Square Errors (RMSE) have also been calculated from the two prediction methods.

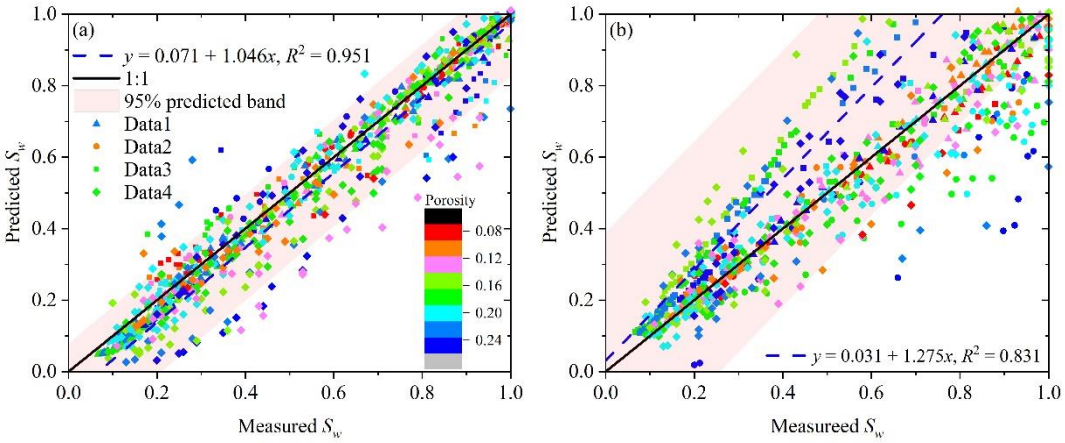

Figure 4. The estimation of saturation based on (a) the new model, and (b) the conventional Archie equation. Samples from different data sets are distinguished by the shape of the symbols. The colours of the symbols indicate sample porosity. The blue dashed line shows the best fit prediction, and should be considered relative to the $y = x$ line.

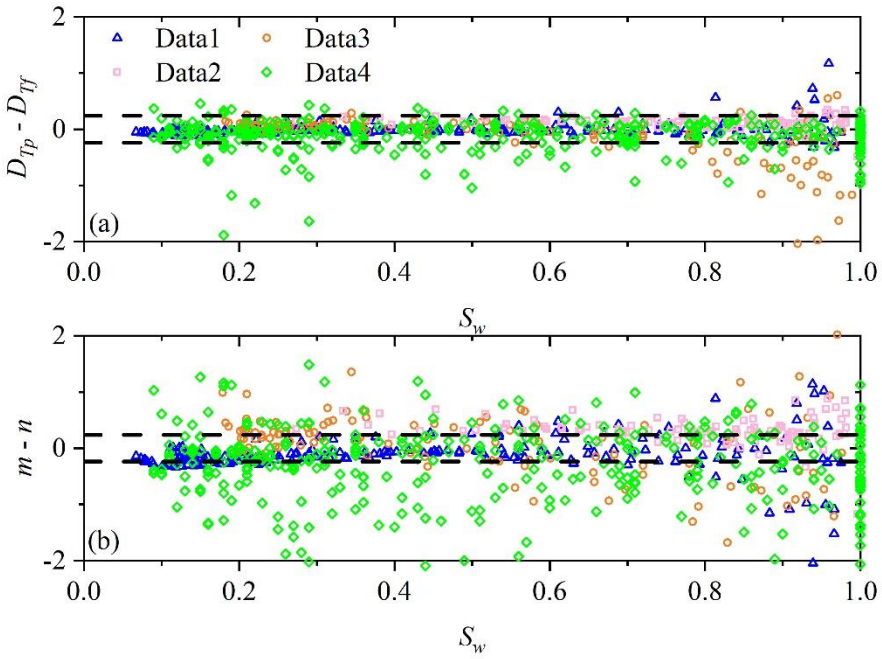

Figure 5. Comparison of (a) D_{Tf} and D_{Tp}, and (b) m and n as a function of S_w. The black dashed lines mark the $\pm 10\%$ error range, respectively.

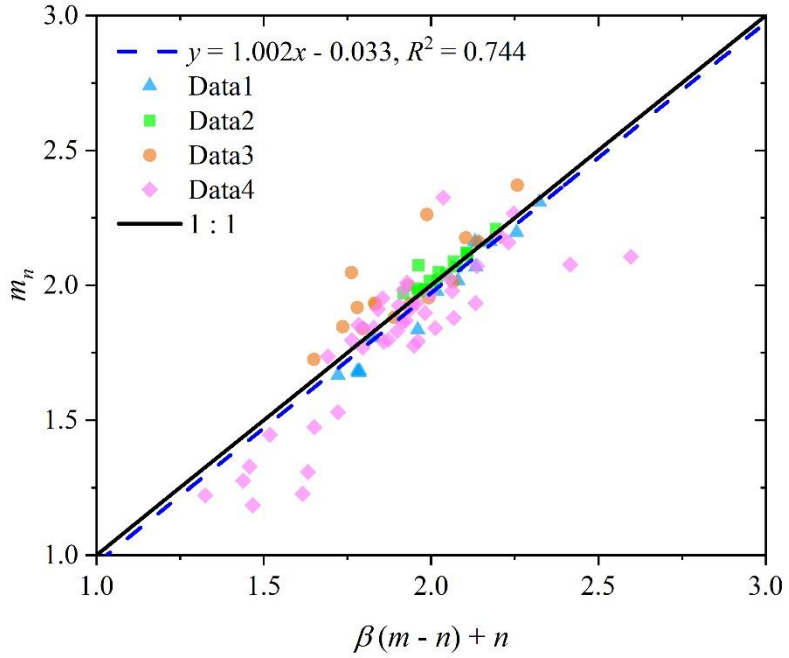

Figure 6. Comparison of the predicted m_n based on Equation (20) and $\beta(m-n)+n$ for each dataset. The measured m is calculated using the formation factor and porosity, and n is determined from the resistivity index and saturation. The blue dashed line represents the best-fit regression, shown against the $y = x$ line for reference.

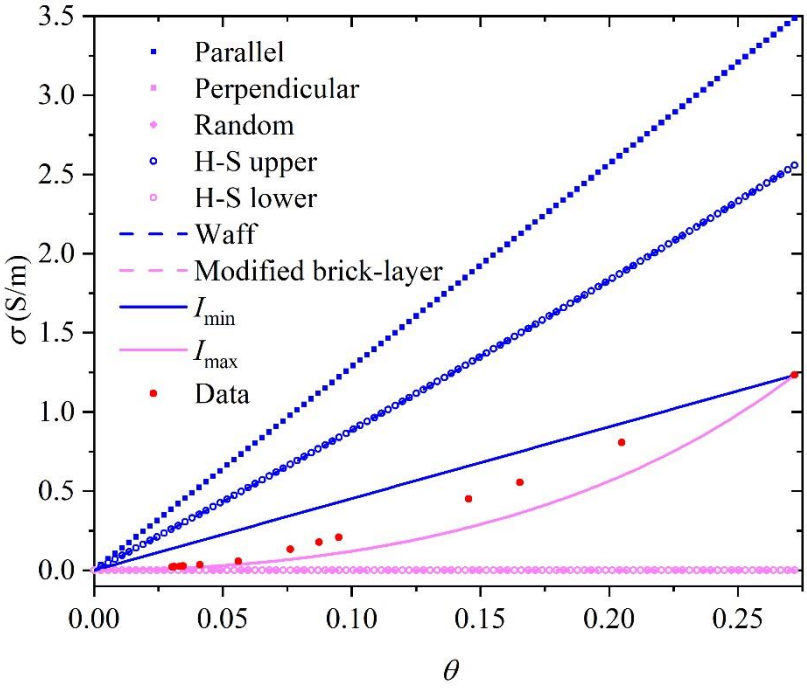

Figure 7. A comparison of the proposed bounds model (where I_{min} and I_{max} from Equation (25) are transformed to electrical conductivity, σ) with other bounds models, showing variation with the content of conducting phase, $\theta = \phi S_w$. The electrical conductivity of conducting phase and non-conducting phase (air and solid) is set at 12.821 S/m and 10^{-7} S/m, respectively. The data is extracted from Data1. Note that the Hashin-Shtrikman (H-S), parallel, perpendicular, random, Waff and modified brick-layer models overlap in this plot.

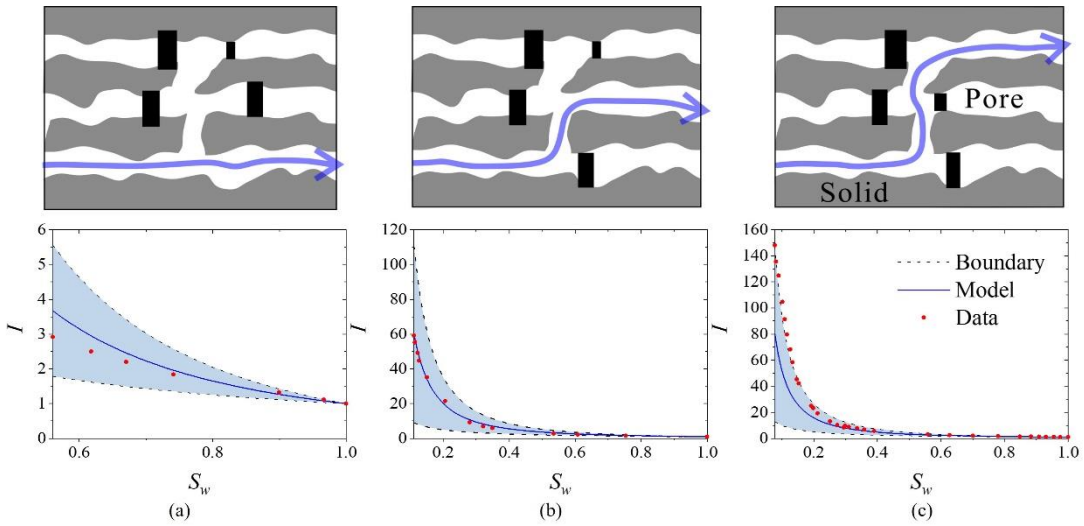

Figure 8. Three forms of tortuous pore space and their resistivity index distribution trend with saturation. (a) Overestimation of the resistivity index in the case of lower tortuosity, (b) accurate prediction of tortuosity and the resistivity index, and (c) underestimation of the resistivity index in the case of higher tortuosity due to the presence of more obstructions. The boundaries are derived from Equation (25) and the model is based on Equation (15) with $D_{Tf} = D_{Tp}$.